

See discussions, stats, and author profiles for this publication at: <https://www.researchgate.net/publication/301581303>

Morphological and clinical characteristics of myopic posterior staphyloma in Caucasians

Article in *Albrecht von Graæes Archiv für Ophthalmologie* · April 2016

Impact Factor: 1.91 · DOI: 10.1007/s00417-016-3359-1

READS

12

5 authors, including:



Rino Frisina

Multizonal Unit Of Ophthalmology of Trento

6 PUBLICATIONS 9 CITATIONS

[SEE PROFILE](#)



Cesana Bruno Mario

Università degli Studi di Brescia

240 PUBLICATIONS 7,152 CITATIONS

[SEE PROFILE](#)



Francesco Semeraro

Università degli Studi di Brescia

121 PUBLICATIONS 1,033 CITATIONS

[SEE PROFILE](#)



Barbara Parolini

Istituto Clinico S.Anna

34 PUBLICATIONS 583 CITATIONS

[SEE PROFILE](#)

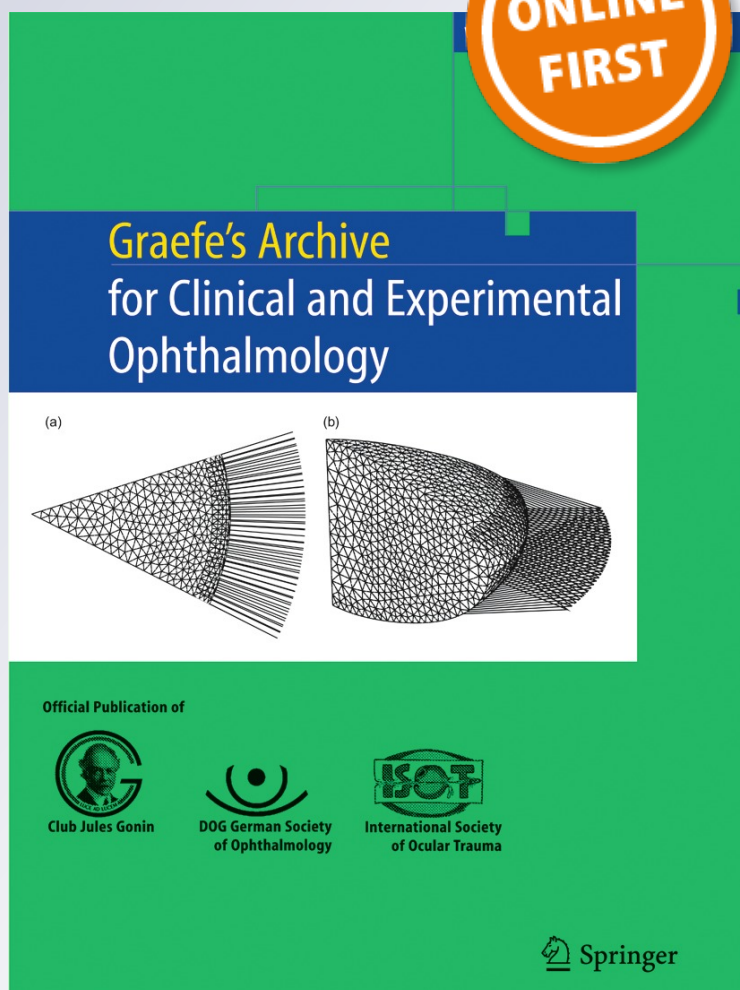
Morphological and clinical characteristics of myopic posterior staphyloma in Caucasians

Rino Frisina, Andrea Baldi, Bruno Mario Cesana, Francesco Semeraro & Barbara Parolini

Graefe's Archive for Clinical and Experimental Ophthalmology
Incorporating German Journal of Ophthalmology

ISSN 0721-832X

Graefes Arch Clin Exp Ophthalmol
DOI 10.1007/s00417-016-3359-1



Your article is protected by copyright and all rights are held exclusively by Springer-Verlag Berlin Heidelberg. This e-offprint is for personal use only and shall not be self-archived in electronic repositories. If you wish to self-archive your article, please use the accepted manuscript version for posting on your own website. You may further deposit the accepted manuscript version in any repository, provided it is only made publicly available 12 months after official publication or later and provided acknowledgement is given to the original source of publication and a link is inserted to the published article on Springer's website. The link must be accompanied by the following text: "The final publication is available at link.springer.com".

Morphological and clinical characteristics of myopic posterior staphyloma in Caucasians

Rino Frisina¹ · Andrea Baldi² · Bruno Mario Cesana³ · Francesco Semeraro² · Barbara Parolini⁴

Received: 23 September 2015 / Revised: 4 April 2016 / Accepted: 14 April 2016
© Springer-Verlag Berlin Heidelberg 2016

Abstract

Purpose We aimed to study the morphological characteristics of myopic posterior staphyloma in Caucasians and to evaluate the correlation between posterior staphyloma, myopic macular lesions and visual acuity.

Methods Ninety eyes of 67 consecutive patients affected by high myopia associated with posterior staphyloma were recruited between January 2012 and December 2013. Posterior staphyloma was classified according to Curtin's criteria. Every patient underwent fundoscopic examination and best corrected visual acuity measurement (BCVA). A and B-scan ultrasound (US), high-resolution, three-dimensional magnetic resonance image (MRI), optical coherence tomography (OCT), fundus autofluorescence (FAF), red free (RF) and color fundus photography studies were performed.

Results The mean age was 64.4 ± 9.48 years (range: 41–82). The mean BCVA was 0.7 ± 0.5 logMAR (range: 0–2). The mean axial length was 29.92 ± 2.39 millimeters (range: 24.25–36.53). The authors found four types of posterior staphyloma according to Curtin's classification: I, II, IV and IX. Significant prevalence of posterior staphyloma in female sex was observed ($p = 0.0235$). Significant correlation

between the depth and the diameters of posterior staphyloma was demonstrated ($p < 0.0001$). Significant association between posterior staphyloma type and tomographic foveal patterns ($p = 0.0230$) was highlighted. Posterior staphyloma type I was more frequently associated with peripapillary atrophy and less with macular atrophy compared to type II and IX ($p = 0.0169$). The prevalence of macular atrophy was more than double in posterior staphyloma type II (33.3 %) in comparison to posterior staphyloma type I (12.5 %).

Conclusions This study confirms that the type I and II are the most common types of posterior staphyloma, as already highlighted in the literature. A significant association between the type of posterior staphyloma and the MRI ocular shape pattern, the OCT patterns of macular profile and the location of chorioretinal atrophy was highlighted. The correlation between the depth and the width of posterior staphyloma has demonstrated that the deeper the staphyloma, the wider it was. The deepest area of the posterior staphyloma was characterized by a greater thinning of the sclera and by a higher prevalence of chorioretinal atrophy compared to the other parts of the eye. More studies are necessary to support our findings and to add more information on the natural evolution of posterior staphyloma and on its associated complications.

Keywords Posterior staphyloma · High myopia · Axial length · Macular retinoschisis · Macular detachment · Myopic traction maculopathy

✉ Rino Frisina
frisinarino@gmail.com

¹ Multizonal Unit of Ophthalmology of Autonomous Province of Trento, corso Verona 4, 38068 Rovereto, Trento, TN, Italy

² Department of Ophthalmology, University of Brescia, Brescia, Italy

³ Biostatistical and Biomathematics Unit, DMMT, University of Brescia, Brescia, Italy

⁴ Department of Ophthalmology, Sant'Anna Institute, Brescia, Italy

Introduction

Myopia is one of the most prevalent ocular disorders and one of the leading causes of visual impairment if not fully corrected [1–6]. Several articles report the prevalence of myopia in different populations. In some Asian countries (China,

Taiwan, Japan and Korea) 80–90 % of children who are completing high school are affected by myopia, and 10–20 % are affected by high myopia [7–9]. The incidence in Americans, which is lower than in Asians, varies between 1 % in Black Americans and 2 % in Caucasian Americans. In North America, there have been studies that confirm a rising incidence of myopia [10, 11].

Pathologic myopia is characterized by several alterations of all the ocular tissues: retina, choroid and sclera. The degree of myopia that defines pathological myopia is not clearly established. However, there is agreement that the spherical equivalent refractive error has to exceed -6 diopters (D) and the axial length (AL) has to be longer than 26.5 millimeters (mm) [12]. Eyes with pathological myopia may show a posterior staphyloma. In 1977, Curtin [13] firstly classified the morphological aspects of posterior staphyloma by fundoscopic examination. He described ten types of posterior staphyloma. Curtin's classification is up to now the main classification used in the clinical practice to define the morphology of posterior staphyloma. In recent studies, the morphological characteristics of posterior staphyloma were observed by using optical coherence tomography (OCT), ultrasound (US) and high-resolution, three-dimensional magnetic resonance imaging (3D-MRI) [14].

Recently, posterior staphyloma was defined by Spaide as 'the ectasia of limited portion of scleral wall with a radius shorter than the radius of the curvature of the surrounding area' [12]. Posterior staphyloma is associated with a high risk to develop macular pathologies such as choroidal neovascularization (CNV), chorioretinal atrophy and myopic traction maculopathy (MTM) [12, 15]. MTM is characterized by macular retinoschisis (MRS), associated or not with one or more of the following complications: lamellar macular hole (LMH), full thickness macular hole (FTMH) and macular detachment (MD) [12, 15].

The aim of this work was to study the morphological characteristics of posterior staphyloma in Caucasian myopic eyes and to evaluate the correlation between posterior staphyloma, myopic macular lesions and visual acuity.

Design

Cross-sectional observational study.

Methods

Every patient affected by high myopia associated with posterior staphyloma, coming to the Department of Ophthalmology of Sant'Anna Institute of Brescia, Italy, from January 2012 to December 2013, was recruited. All patients underwent

ophthalmological examination and best corrected visual acuity (BCVA) measurement using Snellen vision chart and converted into Logarithm of the Minimum Angle of Resolution scale (LogMAR). A and B-scan US, MRI, OCT, autofluorescence (FAF), red free (RF) and color fundus photography studies were performed on all the patients recruited. All eyes with AL longer than 26.5 millimeters (mm) were considered to be affected by high myopia. All patients undergoing episcleral or macular buckling surgery that could cause iatrogenic variation of AL were excluded from this study.

The following clinical parameters were recorded:

- Demographic and functional data: age, sex, eye involved (right or left), status of lens (phakic, pseudophakic, aphakic) and BCVA.
- Type of posterior staphyloma. The posterior staphyloma type was diagnosed by fundoscopic examination, according Curtin's classification criteria and confirmed by US B scan study.
- US parameters: AL, posterior staphyloma width and depth, measured in mm.

AL measurement was performed by hand-held applanation with A-scan US in automatic freeze modality. The values obtained from three consecutive scans, with a difference not exceeding 0.5 mm, were accepted as valid measurements.

The posterior staphyloma width was measured by drawing a line (width line) on a B scan US image from the point where the staphyloma changed the normal posterior pole profile (change in the radius of curvature), until the same point on the opposite part of posterior staphyloma.

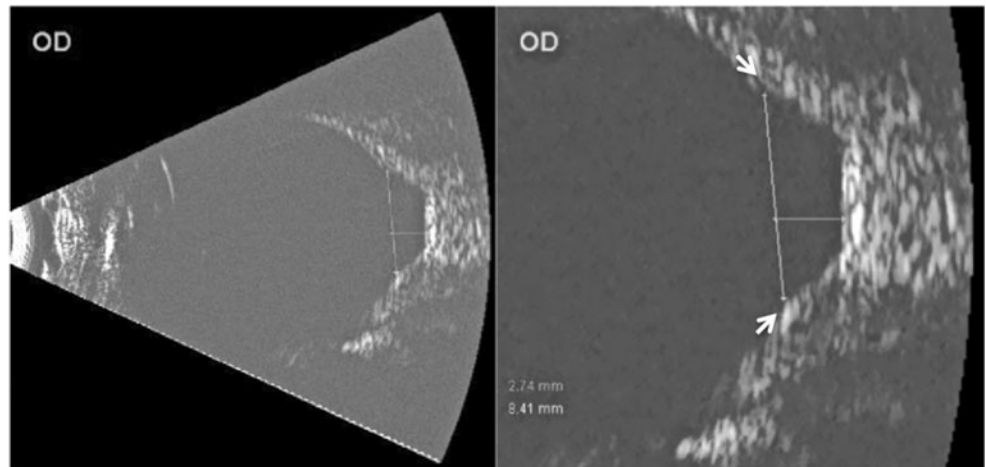
The posterior staphyloma depth was the measured distance between the deepest point into the staphyloma and the width line previously described.

The value of posterior staphyloma width and depth was the mean of three measurements performed on the vertical and the horizontal B scan US images (Fig. 1).

- OCT parameters: scleral thickness, pattern of macular profile.

Scleral thickness was measured on the deepest point of posterior staphyloma. The deepest point was established as the most declive point of macular profile on each OCT scan image. It was measured by OCT caliber in micrometers (μm). Scleral thickness was obtained calculating the mean of three measurements performed on each scan of 12 radial scan images (Fig. 2c). The measurements were performed by Spectral Domain Optical Coherence Tomography (SDOCT), Optovue RTVue (Optovue Inc., Fremont, CA).

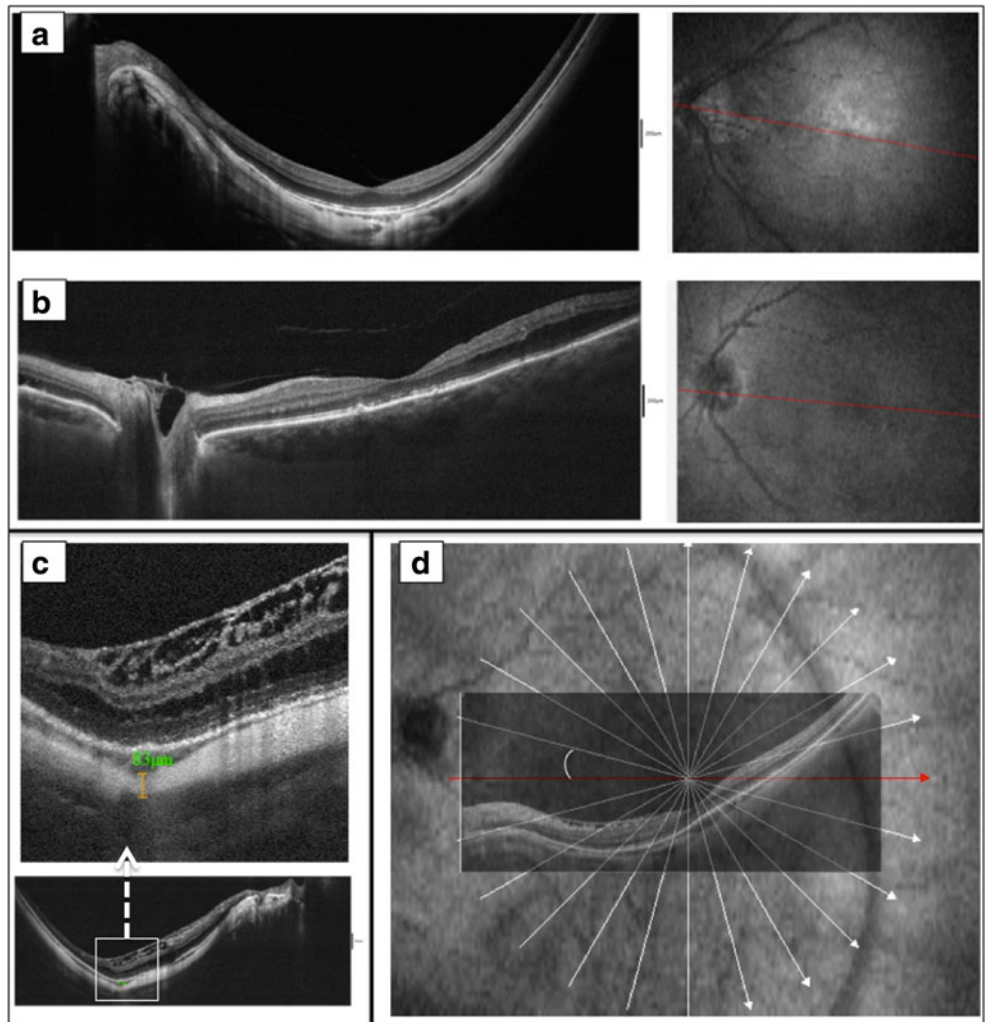
Fig. 1 The figure on the left shows B scan US of posterior staphyloma. The *dashed lines* indicate the diameter and the depth of posterior staphyloma. *White arrows* indicate the points where staphyloma changes the radius of curvature, therefore abruptly changing the expected posterior pole profile. The figure on the right shows the magnified view of the same B scan US with the details of the measures of the diameter and the depth on the area of posterior staphyloma



Pattern of macular profile. The patterns were defined based on position of the fovea into the posterior staphyloma viewing by the OCT scan bisecting the fovea and the optic nerve. The position of the fovea could be at the centre of the posterior staphyloma in the deepest point of the staphylomatic

ectasia or away from the deepest point of staphylomatic ectasia in asymmetric position, sloping on one wall of the staphyloma (Fig. 2a, b). Moreover, if the OCT scan bisecting the optic nerve and the fovea was the horizontal scan, we considered that the fovea was on the same plane

Fig. 2 Pattern OCT of macular profile. **a** Foveal pattern: macular profile with fovea centered in the staphyloma. **b** Temporal pattern: macular profile with fovea sloped toward the optic nerve. **c** Scleral thickness measurement at the deepest point of posterior staphyloma profile (green caliber); continuous line indicates the depth of the staphyloma. **d** The figure shows the most common position of the fovea respect to the optic nerve. The fovea was below the plane of the optic nerve. In this case, the angle between the horizontal OCT scan passing through the fovea and the OCT scan bisecting the fovea and the optic nerve was inferior to 15 degrees



of the optic nerve; otherwise, if it was an oblique scan of the 24 radial scans that was performed, we considered that the fovea was above or below to the plane of the optic nerve depending on the slope of the scan. Each scan of the 24 radial scans differs from the previous by 15 degrees of sloping (Fig. 2d).

- 3DMRI parameter: ocular shape.

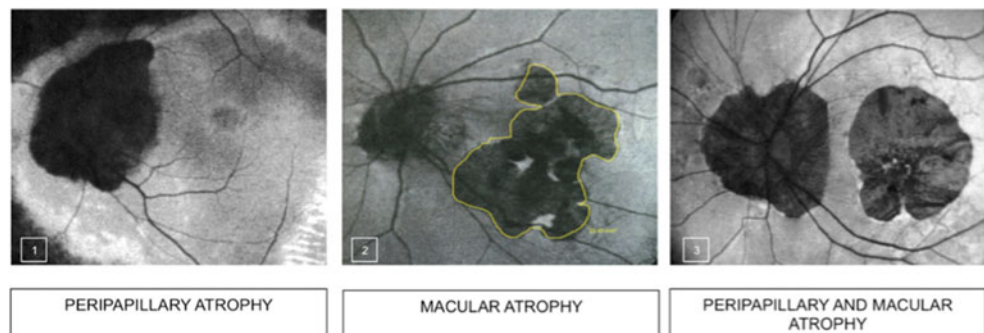
The ocular shape patterns were defined by 3D MRI reconstruction image. T2-weighted image is used to obtain 3D MRI image. The symmetry of nasal and temporal ocular profiles from the superior and inferior view MRI images was analyzed. The symmetry of superior and inferior ocular profiles from the nasal and temporal view MRI images was analyzed. The edges of scleral ectasia from the posterior view MRI image were analyzed.

- FAF/RF/Color Fundus photography. These examinations were performed to localize and measure the extension of chorioretinal atrophic area, measured in μm^2 (Fig. 3).

Statistical analysis

Quantitative variables were described by mean, standard deviation (SD) and minimum and maximum. Qualitative variables were reported as absolute and percent frequencies. Quantitative variables were compared between the staphyloma groups by means of the non-parametric Kruskal-Wallis analysis of variance, followed, in the case of a statistically significant result, by pairwise comparisons between the groups with the Bonferroni's correction. Chi squared test was used for qualitative variables. Correlations between the quantitative variables were carried out by the non-parametric Spearman correlation coefficient. A p value < 0.05 was considered as statistically significant. The statistical analysis was performed by means of SAS 9.2.

Fig. 3 Figure 3 shows the most common patterns of the location of chorioretinal atrophy. In image 2, the Heidelberg software allows the observer to draw a line along the edge of the atrophy (*yellow line*). When the two ends of the line combine, the software calculates the chorioretinal atrophy area (μm^2)



Results

Ninety eyes (45 right and 45 left) of 67 consecutive patients, affected by high myopia and posterior staphyloma, were recruited. Fifty-two were females and 15 were males. The mean age was 64.4 ± 9.48 years (range: 41–82). The mean of BCVA was 0.7 ± 0.5 logMAR (range: 0–2). Only one eye was included in 44 patients. In fact, in 23 of these 44 patients, one eye had undergone macular buckling with or without vitrectomy to treat MTM and the preoperative data could not be recovered. The other 21 among the 44 patients were affected by posterior staphyloma in only one eye. Four of these 21 patients were affected by amblyopia.

The authors found four types of posterior staphyloma: type I in 40 eyes (44.4 %), type II in 39 eyes (43.3 %), type IV in one eye (1.1 %) and type IX in ten eyes (11.1 %) (Fig. 4).

Demographic and functional data for each subgroup of posterior staphyloma are shown in Table 1. Significant prevalence of posterior staphyloma in female sex was observed (Chi square $p=0.0235$). The prevalence of each posterior staphyloma type was reported in Table 1. There was only one case affected by posterior staphyloma type IV and it was excluded from the statistical analysis.

The mean AL was 29.92 ± 2.39 mm (range: 24.25–36.53). The depth of posterior staphyloma was directly related to the horizontal diameter (Spearman's correlation coefficient: 0.4564, $p < 0.0001$) and to the vertical diameter (Spearman's correlation coefficient: 0.4782, $p < 0.0001$) of posterior staphyloma. US parameters are shown in Table 2.

The mean scleral thickness was 160.3 ± 67.28 μm (range: 65–340). The measurements were carried out only on 26 patients, due to the low resolution of the OCT images, which could not ensure the evaluation of the outer edge of the sclera in the other patients (Table 2).

The authors identified two patterns of macular profile:

- Foveal pattern, in eyes where the fovea was in the centre of the posterior staphyloma. The foveal pattern

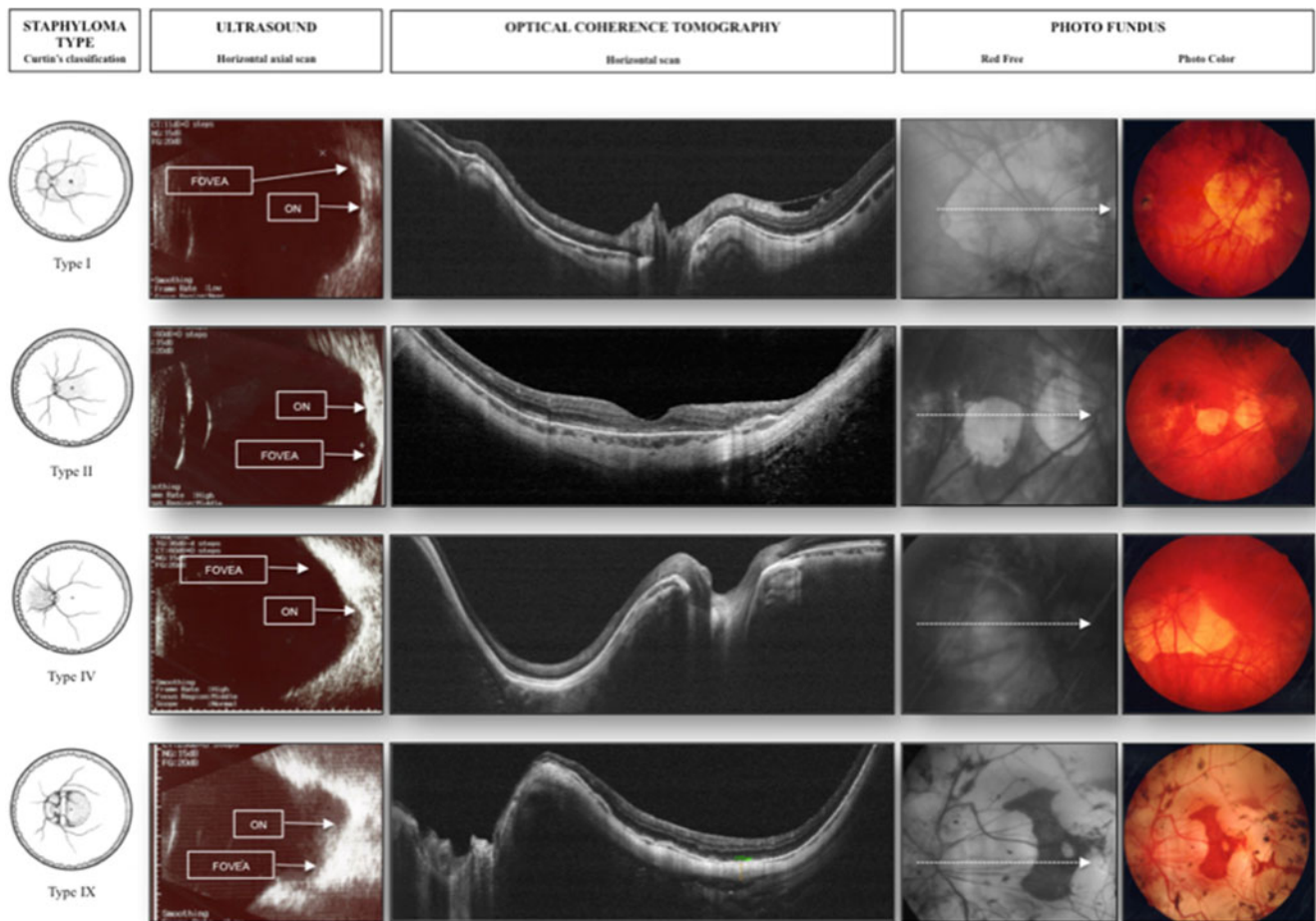


Fig. 4 Posterior staphyloma types: B scan US, OCT, RF and photo color images of posterior staphyloma type I, II, IV and IX

was present in 49 eyes (54.4 %) (Fig. 2a). Three eyes were associated with a dome-shaped macula.

- Temporal pattern, in eyes where the fovea was located on the temporal wall of posterior staphyloma, sloped to optic nerve. The temporal pattern was present in 33 eyes (36.7 %) (Fig. 2b)

In all eyes, the fovea was 10–60 degrees below the plane of the optic nerve.

Seven eyes were affected by MD and it was not possible to identify the pattern of macular profile. One eye was affected by posterior staphyloma type IV, which did not involve the macular area. A significant association between the posterior staphyloma types and the foveal pattern was found ($p=0.0230$). Specifically, excluding the subgroup of posterior staphyloma type IX (nine eyes), the analysis between posterior staphyloma type I and II showed that posterior staphyloma type I was more frequently associated with temporal pattern

Table 1 Demographic and functional data of subgroups of posterior staphyloma type and of whole group of patients

STAPHYLOMA TYPE Curtin's classification	Number of eyes n. (%)	SEX male/female	AGE years mean ± (range)	EYE right/left	BCVA logMAR mean ± (range)
I	40 (44.4)	5/24*	66.06 ± 8.74 52-82	21/19	0.67 ± 0.47 (0–2)
II	39 (43.3)	6/25*	63 ± 9.88 41-78	20/19	0.66 ± 0.37 (0–2)
IV	1 (1.1)	0/1	56	0/1	0.9
IX	10 (11.1)	4/2	64.83 ± 11.6 52-82	4/6	0.92 ± 0.78 (0.1-2)
whole group	90 (100)	15/52	64.4 ± 9.48 41-82	45/45	0.7 ± 0.5 (0–2)
<i>p</i>	-	0.0235*	0.4571	-	0.2932

* χ^2 *p* value (Staphyloma Type IV has been excluded from the analysis)

Table 2 Morphological characteristics of subgroups of posterior staphyloma type and of whole group of patients

STAPHYLOMA TYPE Curtin's classification	Axial Length mm mean \pm (range)	Ultrasound parameters of Staphyloma			Scleral Thickness OCT μm mean \pm (range)	Extension of chorioretinal atrophic area μm^2 mean \pm range
		Horizontal diameter mm mean \pm (range)	Vertical diameter mm mean \pm (range)	Depth mm mean \pm (range)		
I	29.73 \pm 2.16 (24.25–35.97)	14.01 \pm 4.08 (5.59–20.83)	13.62 \pm 3.64 (5.34–23.01)	4.10 \pm 1.45 (0.8–8.43)	147.08 \pm 78.48 (65–325)	611.5 \pm 518.07 (157.80–2020.35)
II	30.11 \pm 2.57 (25.84–36.53)	13.09 \pm 3.15 (2.7–18.7)	13.43 \pm 3.02 (8.1–19.84)	3.92 \pm 1.55 (1–8.62)	170.25 \pm 60.98 (105–340)	611.5 \pm 518.07 (157.80–2020.35)
IV	27.55	8.95	9.54	2.71	–	987.3
IX	30.27 \pm 2.77 (26.63–34.51)	14.39 \pm 4.56 (6.62–22.78)	14.20 \pm 3.95 (7.72–22.72)	4.47 \pm 1.59 (1–8.01)	180 \pm 21.21 (165–195)	981.5 \pm 1073.02 (162.40–2196.16)
whole group	29.92 \pm 2.39 (24.25–36.53)	13.61 \pm 3.77 (2.70–22.78)	13.57 \pm 3.41 (5.34–23.01)	4.05 \pm 1.50 (0.8–8.62)	160.3 \pm 67.28 (65–340)	670.28 \pm 668.8 (102.22–1236.67)
<i>p</i> *	0.7352	0.4580	0.8233	0.5708	0.6569	0.6520

*Kruskall-Wallis Anova

and less with foveal pattern compared to posterior staphyloma type II. Contrarily, posterior staphyloma type II was more frequently associated with foveal pattern and less with temporal pattern compared to posterior staphyloma type I ($p=0.0041$).

MRI was performed in 42 eyes of 21 patients. The authors identified four ocular shape patterns examining the 3D-MRI reconstruction: 'macular distortion' pattern, 'nasal distortion' pattern, 'wide distortion' pattern and 'cylindrical-shaped' pattern. Macular distortion pattern was located only on the macular area (MRI posterior view), with symmetrical nasal and temporal profiles (MRI superior and inferior views). A scleral incision delimited symmetrically the posterior ectasia and the diameter at the level of scleral incision was narrower than the equatorial diameter of the eye. The macular distortion pattern was associated with posterior staphyloma type II. Nasal distortion pattern was characterized by distortion of the scleral wall around the optic nerve (MRI posterior view), with asymmetrical nasal and temporal profiles (MRI superior and inferior views). The asymmetrical profile is due to a scleral incision more accentuated along the temporal profile than nasal profile. The diameter of posterior ectasia was narrower than the equatorial diameter of the eye. The nasal distortion pattern was always associated with posterior staphyloma type I. Wide distortion pattern, involved the optic nerve and macular area, was characterized by asymmetrical nasal and temporal profiles. There was not a scleral incision; however, the asymmetry of the profile was due to an enlargement of ectasia temporally (MRI superior and inferior views) and inferiorly (MRI temporal and nasal views). The diameter of posterior ectasia was equal to the equatorial diameter of the eye. The wide distortion pattern was associated with

posterior staphyloma type I and type IX. Cylindrical-shaped pattern was characterized by a higher elongation of posterior staphyloma with symmetrical nasal and temporal profiles and without a sclera incision along all profiles of MRI views. The cylindrical-shaped pattern was associated with posterior staphyloma type I and type II (Figs 5, 6).

The mean extension of chorioretinal atrophic area into the posterior staphyloma was $670.28 \pm 668.8 \mu\text{m}^2$ (range: 102.22–1236.67). Statistical analysis did not show any significant difference in the extension of chorioretinal atrophy among all subgroups of posterior staphyloma types (Table 2).

The prevalence of location of the chorioretinal atrophic area and the macular profile pattern for each subgroup of posterior staphyloma are reported in figures 7 and 8. There was a statistically significant association between the type of posterior staphyloma and the location of chorioretinal atrophic area ($p=0.0169$). Peripapillary atrophy was the most frequent location, with a prevalence of 87.5 % in posterior staphyloma type I, 66.7 % in type II and 44.4 % in type IX. However, the prevalence of macular atrophy, associated or not with peripapillary atrophy, was more than double in type II (33.3 %, 13 eyes) compared to type I (12.5 %, 5 eyes), although the limited number of eyes did not allow to carry out a statistical analysis. In order to evaluate if BCVA was affected by the location of chorioretinal atrophy, we divided the whole group of eyes into two subgroups: eyes with peripapillary atrophy (63 eyes) and eyes with macular atrophy with or without peripapillary atrophy (25 eyes). The comparison between these two subgroups showed a significant difference ($p=0.0451$); BCVA was worse in eyes affected by macular atrophy (0.95 ± 0.52 , range: 2–0.3 logMAR) than those affected only by peripapillary atrophy (0.7 ± 0.35 , range: 2–0 logMAR).

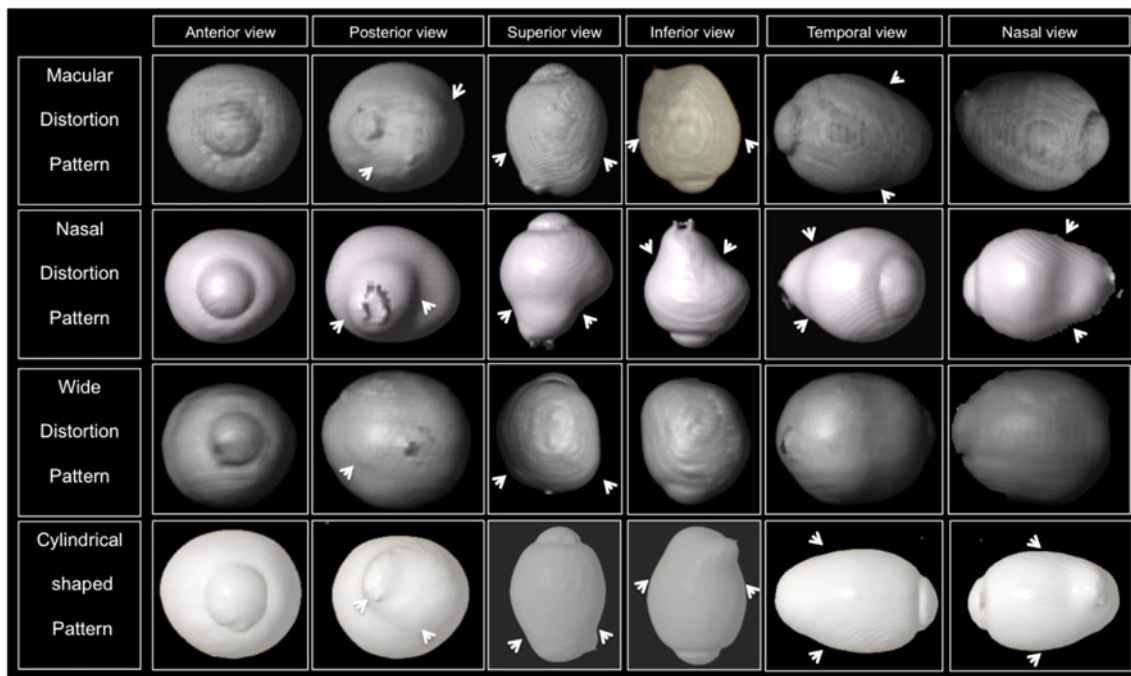


Fig. 5 MRI of ocular shape patterns

The prevalence of retinal pathologies associated with posterior staphyloma was 55.5 % (50/90 eyes). The most common pathology was MTM, which was present in 30 eyes (54.54 %). In 16 cases, MRS was associated with ERM, in five cases with FTMH and in nine eyes with LMH. Seven cases were affected by ERM without MRS. Six cases were affected by choroidal neovascularization. Seven eyes presented MD; four of these were associated with posterior staphyloma type I and three associated with posterior staphyloma type II. The prevalence of MD was 7.7 %. The statistical analysis did not show significant difference in the prevalence of retinal pathologies between the subgroups of posterior staphyloma types (Fig. 9).

Discussion

Prevalence of posterior staphyloma type

In our study, we found that posterior staphyloma type I and II are the most common types, confirming data reported firstly by Curtin [13] and afterwards by other authors [14–17]. Specifically, Hsiang et al. [14] analyzed 209 eyes of 109 Asians and divided them into two subgroups according to their age, respectively under 50 years (younger subgroup) and over 50 years (older subgroup). The most common types of posterior staphyloma, in both groups, were type I and II. Hsiang et al. highlighted that the incidence of posterior staphyloma type IX increases significantly in older patients. In our study, posterior staphyloma type IX was found in only

one eye of one patient younger than 50 years of age and in nine eyes of five patients (four patients in both eyes and one patient in one eye) older than 50 years of age. However, the number of patients in the younger subgroup (eight patients) was lower than the number in the older subgroup (59 patients); therefore, the statistical value of the prevalence of staphyloma IX in the two subgroups of age is not reliable. But we still want to highlight that five of six patients were more than 50 years old, supporting the hypothesis that posterior staphyloma type IX could be more prevalent in older patients.

Ohno-Matsui [17] proposed a new classification of posterior staphyloma based on 3D-MRI reconstruction [17]. She described five types of posterior staphyloma based on the analysis of the outermost border of staphyloma. She revised Curtin's classification, including the five types of combined posterior staphyloma into a single category, and proposed five types of posterior staphyloma corresponding to the first five types of non-combined posterior staphyloma. Ohno-Matsui called posterior staphyloma type I 'wide, macular staphyloma'; type II 'narrow macular staphyloma'; type III 'peripapillary staphyloma'; type IV 'nasal staphyloma'; type V 'inferior staphyloma' [17]. The 'narrow' and 'wide' macular staphyloma were the most common ones [17].

In the light of the results of Ohno-Matsui, we studied the ocular shape of myopic eyes using MRI. MRI allows for study of the ocular shape and not the morphology of posterior staphyloma, because MRI visualizes the external profile of the eye. The internal profile could appear different from the external profile due to MTM that changes the morphology of the staphylomatic ectasia. T2-weighted image is used to obtain

Fig. 6 Descriptive analysis of MRI imaging of three dimensional reconstruction of ocular shape patterns of myopic eyes with posterior staphyloma. *White arrows* indicate the profiles of ocular shape patterns, the sclera incisions along the ocular profiles and the distortions of posterior ectasia described by the authors in the results

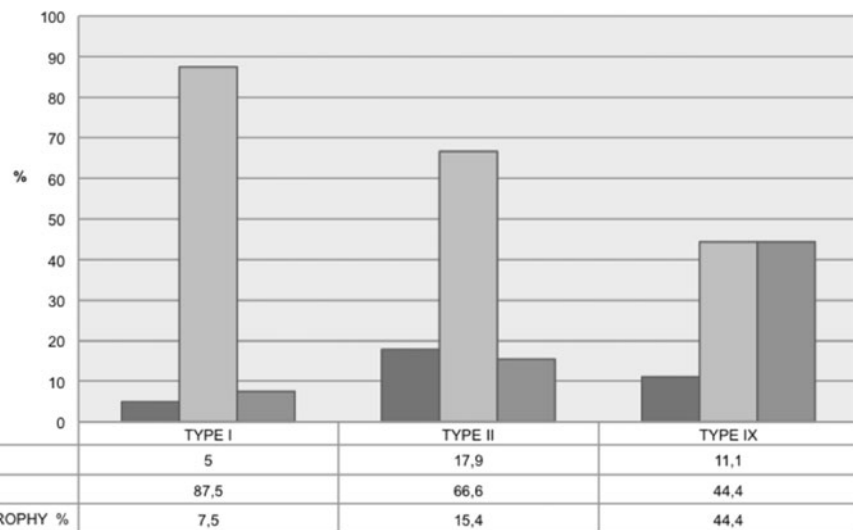
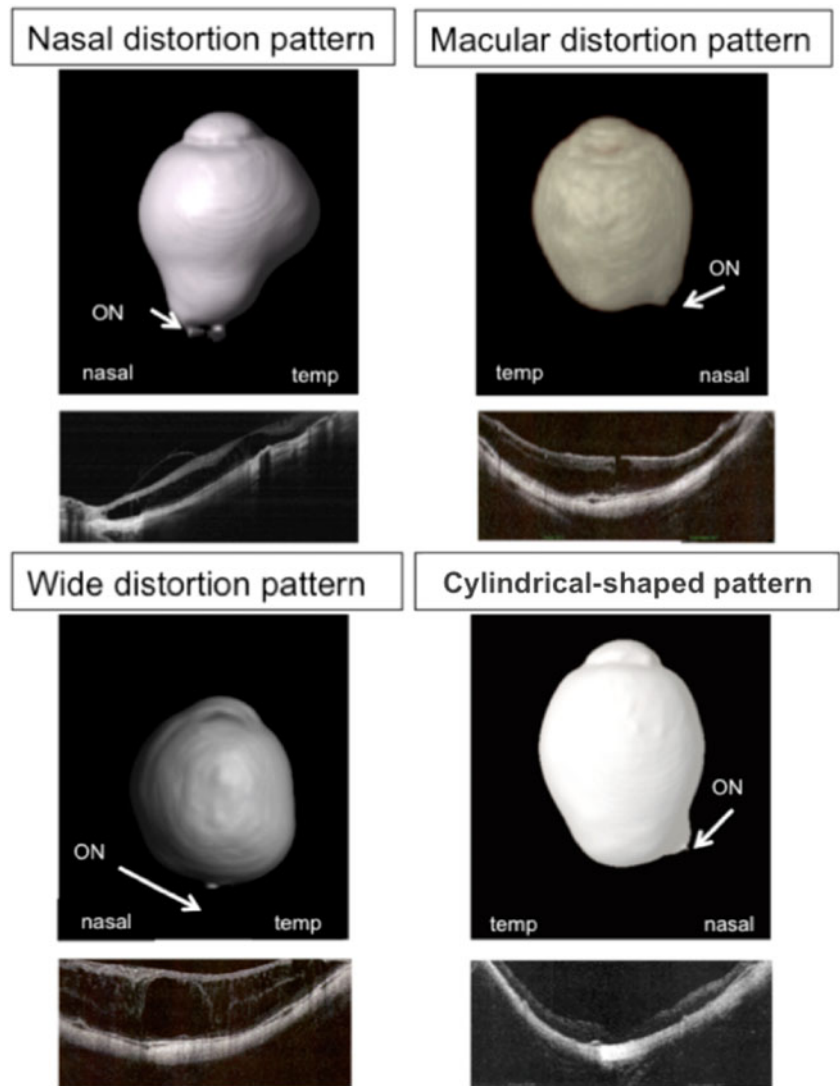


Fig. 7 Prevalence (%) of location of chorioretinal atrophic area in the subgroups of posterior staphyloma type (I, II, IX)

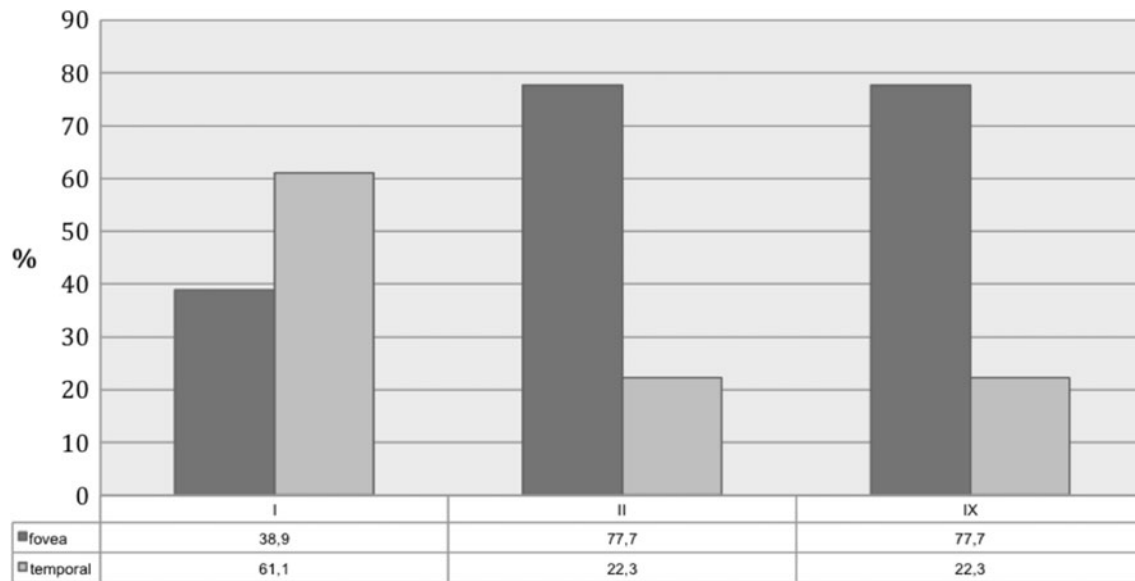


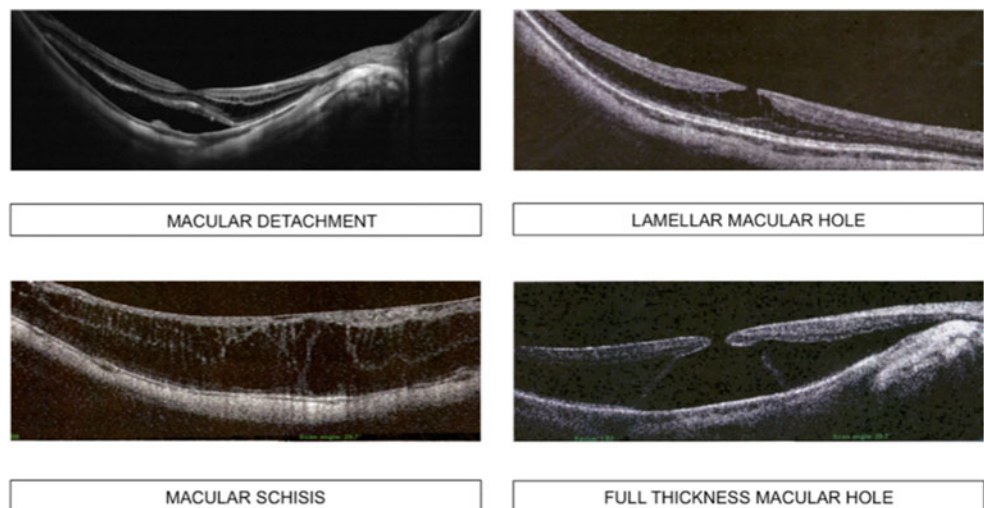
Fig. 8 Prevalence (%) of macular profile pattern (Foveal and Temporal) in the subgroups of posterior staphyloma type (I, II, IX)

3D MRI images, which means that the contour of the eye in 3D MRI image shows the vitreo-retinal interface and not scleral contour. This point should be considered especially in the eyes with retinoschisis and MTM. After defining the patterns of ocular shape, we correlated them with the posterior staphyloma types. Although MRI study allows us to make only a descriptive evaluation of ocular shape without the ability to perform statistical analysis, a few interesting evidences emerged. There are some similitudes between our study and Ohno-Matsui's study. We found that the most common types of ocular shape viewed by MRI were the nasal (44.4 %) and the macular distortion patterns (43.3 %). These two types correspond respectively to posterior staphyloma type I and II of Curtin's classification. Moreover, the MRI morphological characteristics, described by us, nasal distortion and macular distortion pattern, correspond to those described by

Ohno-Matsui, the wide and narrow macular staphyloma, supporting what was previously described [13, 17, 18].

The wide macular distortion pattern was the only one that was characterized by asymmetrical enlargement of staphylomatic ectasia temporally and inferiorly. Ohno Matsui hypothesized that during the development of staphyloma, the ectasia expands more toward the inferior part of the eye [16–18]. The scleral tissue was weaker in the inferior area than in the other areas of the eye, probably due to the fact that the inferior part of the eye is the area of the closure of embryonic ocular fissure. Moreover, wide macular shape was associated with staphyloma IX, which was the one most prevalent in older age and the one most associated with diffuse chorioretinal atrophy. Thus, we hypothesized that the enlargement of the ectasia inferiorly could represent the evolution of the most severe form of myopia.

Fig. 9 Complications associated with myopic traction maculopathy



Evolution of posterior staphyloma

Hsiang et al. [14] followed nine myopic patients affected by staphyloma for a period of 25 years, and noticed an increase of AL and morphological changes of staphyloma during the patients' lifetime. AL increased in all cases. In three cases, posterior staphyloma changed in time from type II to type IX. This morphological change implies an extension of the posterior staphyloma from the macular area, characteristically involved by posterior staphyloma type II, to the optic nerve, involved with the macula by the posterior staphyloma type IX. Our study is an observational cross-sectional study and did not take the time into account as a variable. Therefore we could not evaluate the evolution of posterior staphyloma.

We found, however, a significant correlation between the depth and the diameters of posterior staphyloma. In other words, the deeper the staphyloma, the wider it was. This finding may support the observations of Huang, hypothesizing that during the growth of a posterior staphyloma, there is simultaneously an increase in the diameters and in the depth.

Correlation between macular profile and posterior staphyloma

Ohno-Matsui [16] studied the scleral profile with OCT. She classified four patterns of macular profile. Two patterns were characterized by the accentuation of the normal profile of the emmetropic eye. One of these presented the fovea localized in the centre of the posterior staphyloma and the other type presented the fovea localized in the temporal wall of the posterior staphyloma and sloped towards the optic nerve. The last two patterns were present only in the myopic eyes: one was characterized by the asymmetric localization of the fovea and an asymmetric scleral curvature, the other one was characterized by an irregular scleral contour. We noticed that the first two patterns of macular profile, described by Ohno-Matsui, were the most common, and we called respectively foveal pattern and temporal pattern. The foveal pattern had a prevalence of 69.2 % in type II, where the staphyloma was extended around the macular area. The temporal pattern had a prevalence of 60.6 % in type I. We noticed that the pattern of macular profile is related to the type of posterior staphyloma. Moreover, we found that in the majority of cases, the fovea was located 30–60 degrees below the optic nerve, much more than in the emmetropic eye [18, 19].

Correlation between chorioretinal atrophy and posterior staphyloma

Hayashi et al. [20] hypothesized that chorioretinal atrophy was a consequence of myopic posterior staphyloma and

reported that diffuse chorioretinal atrophy was the most frequently observed maculopathy lesion (60.9 %). Other studies have shown a correlation between macular atrophy, refractive defect and patient age [21, 22]. The study of Chang et al. [22] reported a prevalence of macular atrophy of 19.3 % in a group of patients with myopia of at least 6 D and a prevalence of 42.3 % in a subgroup of subjects with myopia of at least 8 D. In the same study, peripapillary atrophy was present in 81.2 % [22]. In our study, the most common chorioretinal atrophy location was around the optic nerve (peripapillary atrophy), with a prevalence of 73.3 %. There was a relationship between the chorioretinal atrophy location and the posterior staphyloma type. In staphyloma type I, the prevalence of peripapillary atrophy was 95 % (87.5 % of cases with peripapillary atrophy and 7.5 % with peripapillary and macular atrophy). In staphyloma type II, the prevalence of peripapillary atrophy was 81 % (66.6 % of cases with peripapillary atrophy and 15.4 % with peripapillary and macular atrophy). The prevalence of macular atrophy was more than double in type II (33.3 %) compared to type I (12.5 %).

Scleral thickness and posterior staphyloma

Histological studies performed by Curtin have shown that the scleral thickness in the foveal area was 660 μm in emmetropic subjects (AL 22–24 mm) and 233 μm in myopic patients with AL greater than 27 mm [23]. Ohno-Matsui K published, in a series of 246 eyes with pathologic myopia, that scleral thickness in the foveal area was of $227.9 \pm 82.0 \mu\text{m}$ (range 80–546 μm). In our study, we measured the scleral thickness at the deepest point of the posterior staphyloma, regardless of the position of the fovea. Therefore, it was not necessarily the deepest point of posterior staphyloma that corresponded to the fovea. For these reasons, we found that the mean of scleral thickness was 160.3 μm , which is lower than the values that have been reported in previous studies. The authors believe that the deepest point of posterior staphyloma is the area where the sclera is thinnest and consequently the area of greatest weakness of scleral tissue with highest risk for involvement of ectasia.

Correlation of retinal pathologies

In the current study, macular detachment was present in seven of 90 cases, 7.7 %. This result confirm those of Baba et al., who observed foveal retinal detachment with posterior staphyloma in seven of 78 eyes with a prevalence of 9.0 %. OCT revealed no retinal detachment or retinoschisis in any eye without posterior staphyloma [24].

Conclusions

This study confirms that types I and II are the most common types of posterior staphyloma, as already highlighted in the literature. A significant association between the type of posterior staphyloma and the MRI ocular shape pattern, the OCT patterns of macular profile and the location of chorioretinal atrophy was demonstrated. The correlation between the depth and the width of posterior staphyloma has demonstrated that the deeper the staphyloma, the wider it was. The deepest area of the posterior staphyloma was characterized by a greater thinning of the sclera and by a higher prevalence of chorioretinal atrophy compared to the other parts of the eye. More studies are necessary to support our findings and to add more information on the natural evolution of posterior staphyloma and on its associated complications.

Compliance with ethical standards

Conflict of interest The authors certify that they have no affiliations with or involvement in any organization or entity with any financial interest (such as honoraria; educational grants; participation in speakers' bureaus; membership, employment, consultancies, stock ownership, or other equity interest; and expert testimony or patent-licensing arrangements), or non-financial interest (such as personal or professional relationships, affiliations, knowledge or beliefs) in the subject matter or materials discussed in this manuscript.

All procedures performed in studies involving human participants were in accordance with the ethical standards of the institutional and/or national research committee and with the 1964 Helsinki declaration and its later amendments or comparable ethical standards.

For this type of study, formal consent is not required.

Funding No funding was received for this research.

References

1. Resnikoff S, Pascolini D, Mariotti SP et al (2008) Global magnitude of visual impairment caused by uncorrected refractive errors in 2004. *Bull World Health Organ* 86:63–70
2. Junghans B, Kiely PM, Crewther DP et al (2002) Referral rates for a functional vision screening among a large cosmopolitan sample of Australian children. *Ophthalmic Physiol Opt* 22:10–25
3. Kleinstein RN, Jones LA, Hullett S et al (2003) Refractive error and ethnicity in children. *Arch Ophthalmol* 121:1141–1147
4. Lam CS, Goldschmidt E, Edwards MH (2004) Prevalence of myopia in local and international schools in Hong Kong. *Optom Vis Sci* 81:317–322
5. Cumberland PM, Peckham CS, Rahi JS (2007) Inferring myopia over the lifecourse from uncorrected distance visual acuity in childhood. *Br J Ophthalmol* 91:151–153
6. Foster PJ, Jiang Y (2014) Epidemiology of myopia. *Eye* 28:202–208
7. Morgan I, Rose K (2005) How genetic is school myopia? *Prog Retin Eye Res* 24:1–38
8. Pan CW, Ramamurthy D, Saw SM (2012) Worldwide prevalence and risk factors for myopia. *Ophthalmic Physiol Opt* 32:3–16
9. LinLL SYF, Hsiao CK, Chen CJ (2004) Prevalence of myopia in Taiwanese school children:1983 to 2000. *Ann Acad Med Singapore* 33:27–33
10. Katz J, Tielsch JM, Sommer A (1997) Prevalence and risk factors for refractive errors in an adult inner city population. *Invest Ophthalmol Vis Sci* 38:334–340
11. Vitale S, Sperduto RD, Ferris FL 3rd (2009) Increased prevalence of myopia in the United States between 1971–1972 and 1994–2004. *Arch Ophthalmol* 127:1632–1639
12. Spaide RF, Ohno-Matsui K, Yannuzzi LA, eds (2013) *Pathologic Myopia*. New York: Springer; 177–85
13. Curtin BJ (1977) The posterior Staphyloma of pathological myopia. *Trans Am Ophthalmol Soc* 75:67–86
14. Hsiang HW, Ohno-Matsui K, Shimada N et al (2008) Clinical characteristics of posterior staphyloma in eyes with pathologic myopia. *Am J Ophthalmol* 146(1):102–110
15. Yasushi Ikuno and Masahito (2013) *Ohji Retina Chapter. In High myopia and the vitreoretinal complications*. Fifth edn 113, 1912–1919
16. Ohno-Matsui K, Akiba M, Modegi T et al (2012) Association between shape of sclera and myopic retinohoroidal lesions in patients with pathological myopia. *Invest Ophthalmol Vis Sci* 53(10):6046–6061
17. Ohno-Matsui K (2014) Proposed classification of posterior staphylomas based on analyses of Eye shape by three-dimensional magnetic resonance imaging and wide-field fundus imaging. *Ophthalmology* 12(9):1798–1809
18. Moriyama M, Ohno-Matsui K, Hayashi K, Shimada N et al (2011) Topographic analysis of shape of eyes with pathologic myopia by high resolution three-dimensional magnetic resonance imaging. *Ophthalmology* 118(8):1626–1637
19. Rohrschneider K (2004) Determination of the location of the fovea on the fundus. *Invest Ophthalmol Vis Sci* 45(9):3257–3258
20. Hayashi K, Ohno-Matsui K, Shimada N et al (2010) Long term pattern of progression of myopic maculopathy: a natural history study. *Ophthalmology* 117(8):1595–1611
21. Lui HH, Xu L, Wang YX, Wang S et al (2010) Prevalence and progression of myopic retinopathy in Chinese adults: the Beijing Eye Study. *Ophthalmology* 117(9):1763–1768
22. Lan Chang, Chen-Wei Pan, Kyoko Ohno-matsui et al. (2013) Myopia – related fundus changes in Singapore Adults with High Myopia. *American Journal Ophthalmology* 991–999
23. Curtin BJ (1985) Basic science and clinical management. In: *The Myopias*. ; Harper and Row, New York, NY
24. Baba T, Ohno-Matsui K, Futagami S, Yoshida T et al (2003) Prevalence and characteristics of foveal retinal detachment without macular hole in high myopia. *Am J Ophthalmol* 135(3):338–342